Proton radiation-induced enhancement of the dark conductivity of composite amorphous/nanocrystalline silicon thin films

Z. Razieli,[1,*] N. Bosch,[1,*] L. T. Baby,[2] L. Stolik,[1] R. Yohay,[2] R. Rusack,[1] and J. Kakalios[1,†]
[1]*School of Physics and Astronomy, The University of Minnesota, Minneapolis, Minnesota 55455, USA*
[2]*Physics Department, Florida State University, Tallahassee, Florida 32306, USA*

(Received 11 December 2019; revised manuscript received 28 February 2020; accepted 13 March 2020; published 26 May 2020)

While most semiconductor materials are susceptible to radiation damage, we report here an observation of enhancements in the conductivity of undoped composite amorphous/nanocrystalline silicon thin films after irradiation with high-energy protons. When a series of films for which the nanocrystal concentration is varied were irradiated with 16-MeV protons with fluences from 2×10^{13} to 10^{15} protons/cm^2, the dark conductivity following irradiation is increased by up to a factor of 10. Unlike the persistent photoconductivity effect observed in amorphous semiconductors, this enhancement is permanent and is not removed by annealing. Various mechanisms are tested to explain this effect, but none are able to fully account for our observations.

DOI: 10.1103/PhysRevMaterials.4.055604

I. INTRODUCTION

There are unique challenges in designing semiconductor devices that can operate in ionizing radiation environments, such as those encountered in high-energy particle detectors, or satellite-based solar cells [1–3]. Crystalline semiconductors, when irradiated with hadrons, are permanently damaged, leading to degradation in device performance [4–6]. Amorphous semiconductors, where the atoms are randomly arranged, tend to be more radiation tolerant [7–11]; however, their electronic properties, particularly the product of the free-carrier mobility and recombination lifetime, are typically too low for most detector applications [12,13].

Recent studies of thin films of amorphous/nanocrystalline hydrogenated silicon (a/nc-Si:H) have reported enhancements in the dark conductivity and photoconductivity of one to two orders of magnitude for a nanocrystal density well below the percolation threshold [14]. These composite materials might therefore retain the radiation tolerance of a-Si:H, as the crystal fraction in these materials is typically only 2–4%. To test this hypothesis, we have measured the sensitivity of these films to exposure of 16-MeV protons doses up to 10^{15} protons/cm^2. Previous studies of nominally homogeneous a-Si:H have found that ionizing proton irradiation leads to a metastable decrease in the dark conductivity [7,15–17], with the original, preirradiation, dark conductivity being restored when the sample is annealed at temperatures above ∼450 K. In an earlier study, a/nc-Si:H films were irradiated with protons of higher energy than used here, but at lower fluences [18]. This irradiation yielded a metastable decrease in the dark conductivity of roughly an order of magnitude, compared to the preirradiated value. This decrease in the dark conductivity was removed when the film was annealed above 450 K, and the conductivity was restored to its preirradiated value [18]. In contrast, we report below that for a/nc-Si:H exposed to proton fluences above 2×10^{13} cm^{-2}, the dark conductivity increases by as much as a factor of 10, and this enhancement is not removed even after multiple annealing cycles.

A several orders of magnitude increase in the dark conductivity and photoconductivity of nominally homogeneous a-Si:H with proton irradiation has been reported by other groups [19–23]. However, all of these enhancement effects were observed *in situ*, while the film was exposed to a proton beam. Once the irradiation at room temperature was stopped, the dark conductivity and photoconductivity decayed away over timescales ranging from minutes to several days. In contrast, the proton irradiation-induced conductivity enhancement of the composite a/nc-Si:H films described here appears to be a *permanent* change in the materials' charge-transport properties, with no detectible decrease after more than 8 months after the irradiation is stopped.

A photoinduced enhancement of the dark conductivity, termed persistent photoconductivity (PPC), that decays very slowly at room temperature has been observed in certain amorphous semiconductors. Typically, PPC is found in materials where internal structures, such as alternating layers of *n*-type or *p*-type doped a-Si:H [24,25], have potential modulations due to counterdoping (that is, both donors and acceptors are added to the a-Si:H) [25,26], or have compositional morphology, such as a-Si:H containing nanocrystalline germanium inclusions [27]. However the PPC effect is metastable, with the original value of the dark conductivity being restored following annealing at ∼450 K. In contrast, the proton irradiation-induced conductivity enhancement of the composite a/nc-Si:H films described here remains after high-temperature annealing, even after multiple annealing cycles. The creation and characterization of this radiation-induced enhancement effect is the subject of this paper.

*These authors contributed equally to this work.
†Corresponding author: kakalios@umn.edu

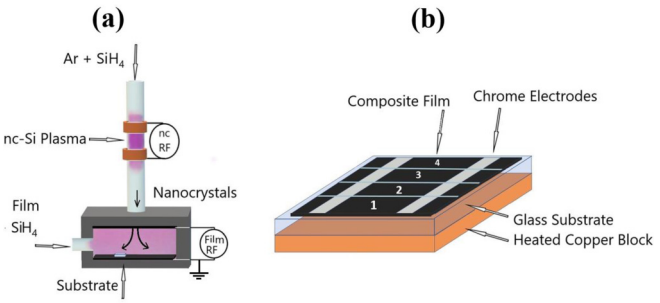

FIG. 1. (a) Schematic of the dual-chamber plasma codeposition system. Due to gas convection within the amorphous semiconductor chamber, there is a gradient of nanocrystal concentration along the sample length. (b) Sketch of the coplanar chrome electrodes scribed into four electrically distinct pads, in order to utilize the nc concentration gradient along the length of the sample. Pad 4 has the highest nc density and pad 1 the lowest.

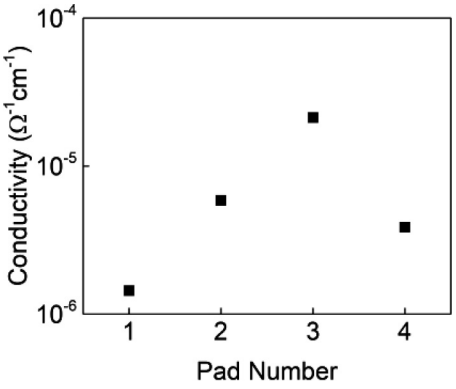

FIG. 2. Plot of the dark conductivity at 450 K of a/nc-Si:H, prior to irradiation, for the four scribed pads as in Fig. 1(b).

This paper is organized as follows. We begin with a brief description of the materials preparation and characterization, followed by a discussion of the proton irradiation processes. The radiation-induced changes in the charge transport in a/nc-Si:H, particularly the dark conductivity, photoconductivity, and sensitivity to light-induced conductivity changes, are compared pre- and postirradiation. We conclude with a discussion and a description of tests we have made to characterize possible mechanisms responsible for this effect.

II. MATERIALS PREPARATION

The undoped composite amorphous/nanocrystalline films were fabricated by plasma-enhanced chemical vapor deposition (PECVD) in a dual-chamber codeposition system, sketched in Fig. 1, and described in detail previously [14]. Briefly, nanocrystals are synthesized in an inductively coupled PECVD chamber, using a flow of silane (SiH_4) and argon. Through control of the chamber gas pressure, agglomerates of nanoparticles are formed, which at high radio-frequency (rf) power are crystallized by electron and ion bombardment. The size of the nanocrystals is determined by the particle residence time in the plasma, which in turn is controlled by the input gas-flow rate and the diameter of the outlet orifice [28–30]. The deposition conditions employed for the fabrication of the samples studied here yielded nanocrystals with diameters on the order of 5–5.5 nm as determined by x-ray diffraction using the Scherrer formula [31]. These nanocrystals are entrained in the flow of argon gas into a second capacitively coupled PECVD chamber, where they become embedded within a surrounding a-Si:H matrix deposited on Corning 1737 F glass substrates heated at 520 K. The elevated substrate temperature enables the silicon atoms to diffuse on the growing film surface in order to find stable, lower defect configurations, which improve the film's quality. Gas convection in the second chamber leads to a concentration gradient of nanocrystals embedded within the a-Si:H along the substrate's length [14]. The substrate is oriented in the deposition chamber so that one end is near the particle injection tube and has the highest nc concentration, while the other end of the substrate, farthest from the injection tube, has the lowest nc content.

Electrical contact is made by evaporating 100-nm-thick chrome coplanar electrodes (length 1.0 cm, separation 0.1 cm) onto the composite a/nc-Si:H thin film, as shown in Fig. 1(b). These electrodes exhibit linear current-voltage characteristics for all of the samples and temperatures investigated here. The samples are scribed across the width of the electrodes [Fig. 1(b)] yielding four distinct 2.5-mm-long pads, with an approximately uniform nanocrystal concentration within each pad. The pad farthest from the particle injection tube with the lowest nanocrystal concentration is designated pad 1, while the part of the substrate closest to the injection tube with the highest nanocrystal concentration is labeled pad 4. Prior studies using Raman spectroscopy measurements described in detail later have found that typically the silicon crystal content X_c for pad 4 to be ∼10%, while for pads 2 and 3 $X_c \sim 2-4\%$ and for pad 1 it is less than 1% [14].

The dark conductivity of the a/nc-Si:H films increases nonuniformly with nanocrystal content, as reported previously [14]. Figure 2 shows the dark conductivity at 450 K of the four pads on a single substrate for an a/nc-Si:H film prior to proton irradiation. The highest conductivity is found for pad 3, which has a crystal content of 2–4%, even though pad 4 has a higher crystal content. The larger conductivity values for pads 2 and 3 are due to modulation doping, where a thermally excited electron in a nanocrystal is able to easily move into the a-Si:H matrix, increasing the film's conductance. The band offset between the nc and a-Si:H is only ∼0.1 eV for the conduction band, while it is ∼0.3 eV for the valence band [32], and the thermally excited holes remain in the nanocrystal. The decrease in the dark conductivity of the pad 4 films relative to pad 3 is accounted for by an increase in dangling bond density in films with higher nanocrystal content, as determined by optical absorption and electron paramagnetic resonance measurements [14,33]. These excess defects trap the electrons promoted from the embedded nanocrystals and decrease the magnitude of the modulation doping effect.

Previous studies of the intentional oxidation of freestanding nanocrystals, synthesized via plasma-enhanced CVD as in Fig. 1, find that the surface of the nanocrystals is hydrogen terminated [34,35]. Using electron spin resonance (ESR) and Fourier transform infrared spectroscopy (FTIR), these authors find that oxide growth on the nanocrystal surface proceeds quite slowly in atmosphere, and in fact is stable against surface

oxide formation for many hours of air exposure. However, they do report a weak signal in both ESR and FTIR consistent with a small amount of oxygen contamination of the nc, perhaps due to *in situ* etching of the Pyrex reactor tube when operated at the high-rf power levels necessary for nc formation.

III. PROTON IRRADIATION

The samples were irradiated with 16-MeV protons at the John D. Fox 9 MV Tandem van de Graaf Accelerator at the Florida State University (FSU). The beam intensity was varied between 1 and 10 nA, which at the upper current level corresponds to 6.3×10^{10} protons per second. The proton beam was defocused with a transverse width of ∼9 mm, in order to irradiate the maximum number of the pads at once. The sample was positioned so that pads 2, 3, and 4 received a nearly uniform exposure. Irradiation times and currents were increased to achieve proton doses of 2×10^{13} p/cm^2, 2×10^{14} p/cm^2, and 10^{15} p/cm^2 for three separate (nominally identical) samples, respectively.

During the irradiation the sample was mounted on a copper support plate and placed in a vacuum chamber, where the pressure during the irradiation was 10^{-6} Torr. The sample bridges a hole in the support plate that allows protons to pass through the sample without activating the copper. The 100-nm-thick chrome electrodes deposited on top of the 1-μm-thick a/nc-Si:H film are irradiated along with the sample. For the proton energies employed here, the chromium-52 (Cr-52) undergoes a (*p,n*) reaction to manganese-52 (Mn-52), which is radioactive with a half-life of 5.59 days. Based on the reaction cross section for the (*p,n*) reaction and half-life of the nuclei produced, we estimate a decay activity of ∼52 decays per second on a 100-nm chrome layer, which is reduced to negligible levels in a few weeks, at which point the samples were first measured postirradiation.

The copper stand on which the sample was secured in the irradiation chamber was in turn mounted on an ethanol-chiller stage (base temperature 262 K) to remove heat from the beam interactions. The energy lost by 16-MeV protons in 1 micron of silicon is 5.5 keV [36]. In the 1.0-mm glass substrate the energy lost was 6.6 MeV, yielding a heating rate of 66 mW for a beam current of 10 nA. Using two platinum-100 resistance thermal sensors, placed a few centimeters from the sample, it was estimated that for the largest fluence, which required the longest irradiation time, the temperature rise of the sample above the ambient room temperature was much less than 100 K. As the films were deposited at 520 K, this temperature increase during irradiation alone is not expected to induce irreversible changes in the material's properties.

IV. EXPERIMENTAL RESULTS

To measure the dark conductivity of the a/nc-Si:H film before irradiation, the sample is mounted in a vacuum chamber on a copper block in which resistive heaters are embedded, and electrical contact is made to one pair of the four scribed electrode pads [Fig. 1(b)]. The film is first annealed at 470 K for 2 h under vacuum (∼1 mTorr) in order to remove any light-induced defects [37,38] or surface adsorbates such as water vapor [39] that could induce a surface charge and band bending in the thin films. The conductivity is then measured as a function of temperature on cooling to 300 K. The vacuum chamber is opened so that the leads can be moved to another of the four pads on the sample, at which point the above procedure is repeated. This process is carried out for all four pads on three separate samples that are deposited under nominally identical conditions. These three samples were then brought to the FSU proton beam irradiation facility, where they were irradiated and then returned to the laboratory in Minnesota, where the samples were remeasured using the same procedures employed before irradiation.

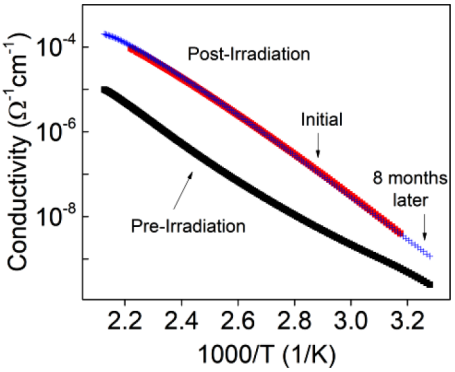

FIG. 3. Arrhenius plot of the dark conductivity of a film prior (black solid squares) and after (red solid squares) irradiation with a fluence of 10^{15} cm^{-2} high-energy protons. The sample was remeasured 8 months later (blue crosses).

Figure 3 shows an Arrhenius plot of the pre- and postirradiated dark conductivity of an a/nc-Si:H film that has been exposed to a dose of 10^{15} protons/cm^2. The black data points represent the conductivity of pad 4 on an a/nc-Si:H film before irradiation, while the red solid squares are for the same film and pad shortly after irradiation. There is an increase in the dark conductivity of over an order of magnitude at 450 K, even after multiple annealed cycles. The same measurement was repeated 8 m later (blue crosses) and an identical enhancement was observed. There is no significant change in the conductivity, indicating that the enhancement of the dark conductivity with irradiation is permanent.

This enhancement of the dark conductivity is found in all of the pads on a given sample. The dark conductivity at 450 K of the series of a/nc-Si:H films with increasing nc content is shown in Fig. 4, both before (black open squares) and after proton irradiation (red solid squares) for a proton dose of 10^{15} cm^{-2}. The preirradiation conductivity values are the same as in Fig. 2. Following irradiation and annealing, the dark conductivity is increased for all three samples investigated.

As shown in Fig. 5, the dark conductivity of pad 4, which has the highest nanocrystalline concentration, increases with the proton dose, and for the highest dose studied, the dark conductivity after irradiation is over an order of magnitude larger above the initial, preirradiation conductivity value. While the ratio of postirradiated to the preirradiated conductivity is nonmonotonic, the absolute values of the postirradiated conductivities increase linearly with dose as can be seen in

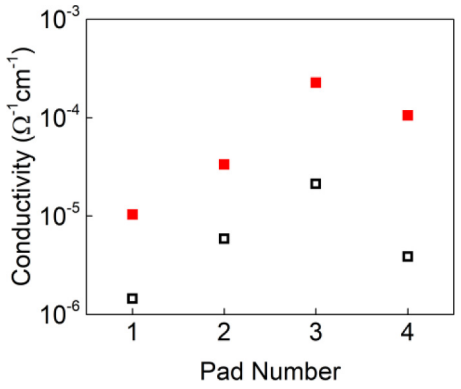

FIG. 4. Plot of the dark conductivity, measured at 450 K, of an a/nc-Si:H film prior to irradiation (open black squares) and after (solid red squares) with a fluence of 10^{15} cm^{-2}, for the four scribed pads as shown in Fig. 2.

Fig. 5. For Figs. 3–6, the errors bars in the measurement of the conductivity are smaller than the size of the plotted data points.

The ability to deposit a-Si:H as a thin film over large areas on a wide variety of substrates makes it an attractive material for photovoltaic applications. However, extended illumination of a-Si:H with absorbing white light leads to the creation of excess metastable dangling-bond midgap defects, termed the Staebler-Wronski effect (SWE) [37,38]. These light-induced defects act as additional recombination centers, decreasing the photoconductivity, and also move the Fermi energy towards the midgap due to a statistical shift, decreasing the dark conductivity. That is, upon termination of the light soaking, the dark conductivity does not return to its original value, but can be several orders of magnitude lower, depending on the magnitude of the Fermi energy shift. The light-induced defects are removed upon annealing above 450 K, at which point the original dark conductivity and photoconductivity are restored, and the process can be repeated. The SWE leads to a light-induced decrease in the photoconversion efficiency of a-Si:H-based solar cells and photodetectors. Reports that embedding silicon nanocrystalline inclusions in a-Si:H reduces the magnitude of the SWE was in part the motivation

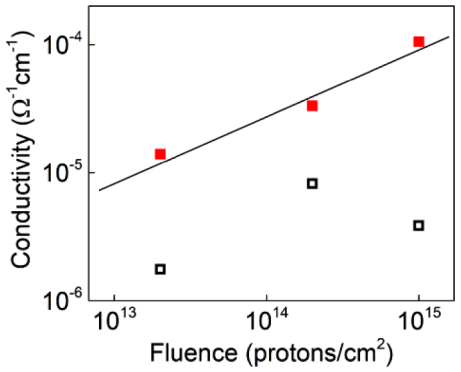

FIG. 5. Plot of the dark conductivity at 450 K of pad 4 for three separate a/nc-Si:H samples as a function of proton dose (red solid squares). The line is a guide to the eye. For comparison the dark conductivity before irradiation (black open squares) is also shown.

for the construction of the dual-chamber codeposition system shown in Fig. 1. As the optoelectronic properties of a-Si:H are of interest for technological applications, we have used our irradiated samples to investigate how the SWE of a/nc-Si:H is affected by proton irradiation.

We first describe the measurement procedure to characterize the SWE of the a/nc-Si:H films in the preirradiated state. The samples were annealed under vacuum in the dark at 470 K for 2 h, and then cooled to room temperature. Using terminology introduced by Staebler and Wronski [37,38], the sample in this annealed state is labeled "state A." The photoconductivity is then measured using a heat-filtered W-Ha lamp (intensity $\sim$75 mW/cm^2) over a 2-h interval. This places the sample into "state B," again using the conventional labeling for the SWE, and the dark conductivity of state B is remeasured as the sample is again annealed to 470 K. At this temperature the light-induced changes in the conductivity (state B) are removed, and the sample is returned to state A. The temperature dependence of the restored state A dark conductivity is then measured once again upon cooling to room temperature. This procedure was repeated for the postirradiated films, approximately 8 m after the irradiation.

The ratio (R_{SW}) of the dark conductivity in the light-soaked state B to that in the annealed state A at 305 K is shown in Fig. 6(a) for pad 4 for the three samples as a function of radiation dose, before (open black squares) and after (solid red squares) the irradiation. If there were no light-induced changes, then R_{SW} should be unity. A ratio less than 1 reflects a light-induced decrease of the dark conductivity (SWE), that is the conductivity in state B$<$state A, while a ratio greater than 1 is a persistent photoconductivity effect. These light-induced changes in the dark conductivity are removed upon annealing at 470 K, unlike the permanent enhancement of the dark conductivity observed with proton irradiation (Fig. 3).

The photoconductivity measured as soon as illumination begins (before any significant increase in the density of light-induced defects), for both the pre- (open black squares) and postirradiated (solid red squares) states at 305 K are shown in Fig. 6(b) for pad 4 as a function of radiation dose. It is important to note that the data in Figs. 6(a) and 6(b) for the postirradiated films were obtained 8 m after the irradiation, and after the samples had been annealed under vacuum multiple times. Consequently, any metastable defects created at the time of proton irradiation would have been annealed away when the data in Fig. 6 were acquired.

The data for the preirradiated ratio R_{SW} of the state B/state A dark conductivity (open squares) for the three samples in Fig. 6(a) display a sample-to-sample variation, as also observed in other a/nc-Si:H samples fabricated at the same time as those in Fig. 6, and were reported previously [14]. The preirradiated values plotted in the figure correspond to the particular samples that were exposed to a given high-energy proton dose. There is no significant change in the sensitivity to light-induced defect creation for the irradiated films, compared to the a/nc-Si:H films measured prior to irradiation.

V. DISCUSSION

As described above, we observe an enhancement in the dark conductivity of a/nc-Si:H when the samples are

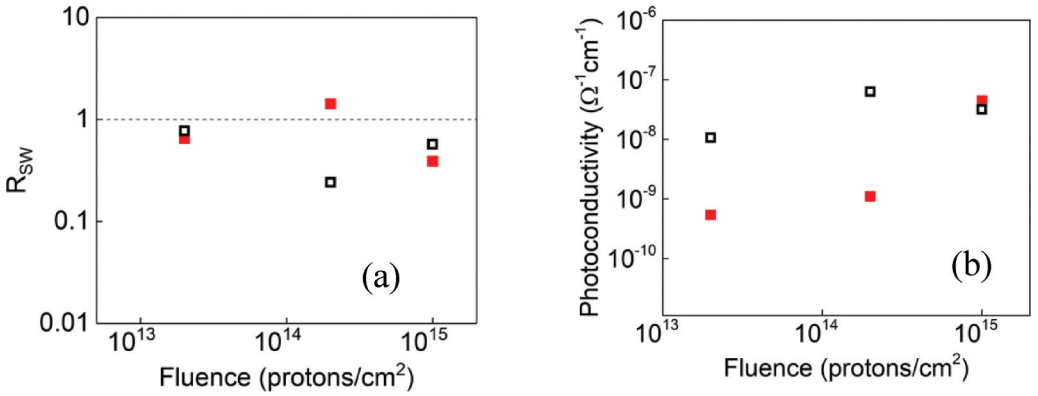

FIG. 6. Plot of (a) the ratio R_{SW} of the dark conductivity following light soaking (state B) to the dark conductivity after annealing (state A) and (b) the initial photoconductivity of a/nc-Si:H at 305 K for pad 4 before (open black squares) and after (solid red squares) proton irradiation as a function of high-energy proton dose.

irradiated with 16-MeV protons for fluences $\geqslant 2 \times 10^{13}$ cm^{-2}. Unlike the photoinduced conductivity enhancements observed in a-Si:H-based structures, this increase in the dark conductivity is permanent with no significant variation observed in the enhanced conductivity over a period of 8 m after multiple annealing cycles.

While surprising, the observation of an enhancement of the dark conductivity with irradiation is not unprecedented. Flitsiyan *et al.* [40] found a permanent increase in the conductivity of ZnO films with neutron exposure with a maximum dose of 7×10^{17} cm^{-2}. They attributed this to a combination of an increase in the free-carrier density, due to the creation of electrically active interstitial Zn, and an enhancement of the mobility, resulting from an improvement in the lattice crystallinity, as reflected in a reduction in the cathodoluminescence signal.

The dark conductivity σ of an amorphous semiconductor is given by $\sigma = nq\mu$, where n is the density of charge carriers excited to the conduction- or valence-band mobility edge, q is the electric charge, and μ is the free-carrier mobility. Thus, as in the case of the neutron-irradiated ZnO, a permanent increase in the dark conductivity in a/nc-Si:H must result from an increase in n or μ, or a combination of the two. However, the results described below do not provide consistent support for an increase in either of these properties.

Charge transport in undoped a-Si:H is predominately n type [12], and the electron free-carrier density is given by $n = N_C(E_C)\,kT\exp[-(E_a/kT)]$, where $N_C(E_C)$ is the density of states at the conduction-band mobility edge E_C, the activation energy is $E_a = E_C - E_F$, where E_F is the Fermi energy, k is Boltzmann's constant, and T is the temperature. An increase in the density of charge carriers n would be reflected by a decrease in E_a.

Table I lists the difference in the measured $\Delta E_a = E_a$(preirradiation)-E_a(postirradiation) in the temperature range of 390–450 K. A negative ΔE_a indicates that the measured activation energy after irradiation is larger than that measured before proton exposure, which should result in a decrease of the dark conductivity. An increase in the conductivity by a factor of 10 at 450 K following irradiation would suggest a decrease of E_a of ~0.09 eV. Arrhenius plots with $\Delta E_a < 0$ exhibit crossings of the pre- and postirradiation conductivity curves near room temperature. Many films exhibit curvature on the Arrhenius plot, such as found in Fig. 3, suggesting that a simple thermally activated expression is not the best description of the conductivity temperature dependence. While in some cases the measured activation energy shift is of the right order to account for the change in conductivity, it is not consistent for all the samples measured. This suggests that the enhancement is more complex than a simple shift of the Fermi energy following irradiation and might be due to an increase in the conductivity prefactor $\sigma_o = N_C(E_C)kTe\mu$. If the enhancement of the σ is due to an increase in $N_C(E_C)$ in the conductivity prefactor, this would suggest that the conduction-band edge moves to higher energies. Such a shift would increase the activation energy (if the Fermi energy remains at its original position in the mobility gap) that would in turn decrease the conductivity. We next consider the possibility that this enhancement is due to an increase in the free-carrier mobility μ.

TABLE I. Ratio of dark conductivity σ for a/nc-Si:H films measured at 450 K after (post-) and before (pre-) proton irradiation and the change in measured activation energy ΔE_a as a function of proton fluence.

Proton fluence (cm^{-2})	Pad 4		Pad 3		Pad 2		Pad 1	
	$\frac{\sigma_{post}}{\sigma_{pre}}$	ΔE_a(eV)	$\frac{\sigma_{post}}{\sigma_{pre}}$	ΔE_a(eV)	$\frac{\sigma_{post}}{\sigma_{pre}}$	ΔE_a(eV)	$\frac{\sigma_{post}}{\sigma_{pre}}$	ΔE_a(eV)
10^{15}	27.4	0.09	10.7	0.08	5.7	−0.12	7.2	−0.17
2×10^{14}	4.0	0.06	13.3	0.12	4.2	0.02	12.8	−0.17
2×10^{13}	7.9	0.34	4.8	0.13	22.5	−0.04	4.3	−0.16

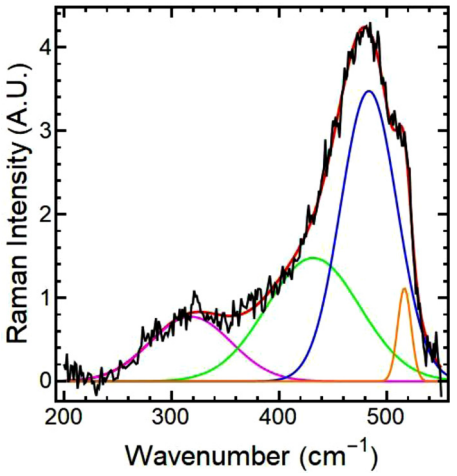

FIG. 7. Plot of the Raman-scattering intensity against wave number for an a/nc-Si:H film (pad 4) after irradiation for a dose of $10^{15}\,\mathrm{cm}^{-2}$. The curve is fit (red line) using the known peak locations for the a-Si:H LA (purple curve), LO (green curve), and TO (blue curve) modes and the c-Si TO (gold curve) mode.

The mobility in a-Si:H is on the order of $\sim 10\,\mathrm{cm}^2/\mathrm{V\,s}$, which corresponds to an inelastic scattering length of <1 nm [41,42]. The silicon crystal fraction in the films that were irradiated is $\lesssim 7\%$, corresponding to a nanocrystal density far below the percolation threshold. For nanocrystals with a diameter of 5.5 nm, this corresponds to a density of nanocrystals of $\sim 3 \times 10^{17}\,\mathrm{nc/cm}^3$, which in turn indicates an average separation of nc of ~ 15 nm. Thus, the mobility in these films prior to irradiation should be comparable to that of pure a-Si:H.

An order of magnitude increase in the mobility would imply a corresponding increase in the inelastic scattering length to >10 nm, which has never been observed in a-Si:H, and in fact is comparable to scattering lengths in polycrystalline silicon [12]. It is possible that the energy deposited in the film by the 16-MeV protons leads to crystallization of the surrounding a-Si:H matrix, with this process potentially occurring preferentially at the nc inclusion sites. We have taken precautions, described in Sec. III, to avoid heating of the films by the proton beam. However, transmutation of some nuclei in the chrome electrodes during proton irradiation into radioactive Mn-52, with a decay mode primarily of positron emission, is possible. Earlier studies of proton irradiation of a/nc-Si:H at lower fluences [18] did not find an enhancement of the dark conductivity, even though these films also had chrome electrodes with the same geometry as used in the films reported here. Nevertheless, localized heating cannot be definitively excluded, such that irradiation results in an increase in the amount of material in the nc phase, either by increasing the number of nanocrystals or their average size (or a combination of the two). In that case, the composite films could be considered as two resistors in parallel, and the growth of the nc phase would lead to more current being able to flow through the nanocrystals, increasing the conductance of the composite film.

To test this, we have measured the Raman spectra of the irradiated films, using a 514.5-nm argon ion laser at a power of less than 6 mW, with care taken to avoid heating of the films. Figure 7 shows the measured Raman spectrum for pad 4 of the a/nc-Si:H film irradiated with a dose of $10^{15}\,\mathrm{cm}^{-2}$. Noteworthy features are the broad peak at $480\,\mathrm{cm}^{-1}$, associated with the a-Si:H TO Raman mode, and a smaller peak at $\sim 518-520\,\mathrm{cm}^{-1}$ that is the TO mode in crystalline silicon [43]. The fit at lower wave numbers is obtained by including the a-Si:H LA and LO modes. The crystal fraction can be determined from the relative amplitudes of the c-Si (I_{520}) and a-Si:H (I_{480}) TO modes, $X_c = I_{520}/(I_{520} + I_{480})$, where we have taken the relative Raman scattering cross sections for the crystal and amorphous phases to be equal. The data in Fig. 7 indicate that $X_c = 7\%$ for this pad.

Table II lists the average X_c values obtained, as for Fig. 7, for all three samples that were irradiated, averaged for multiple locations within pad 4, as well as for pads 3, 2, and 1. There is no appreciable c-Si TO mode observed in pads 1 and 2, even though these pads also exhibited a significant conductivity enhancement. Pad 4 shows an average crystal fraction of $\sim 6-7\%$ regardless of the proton fluence, while there is a significant difference in the conductivity enhancement. If the permanent increase in the dark conductivity is indeed associated with a growth of the nc phase with proton irradiation, the connection between the nc density and the conductivity is not straightforward or monotonic. In addition, the mechanism by which the nc concentration increases, without a significant rise in the temperature during irradiation, would need to be determined.

An enhancement of several orders of magnitude of the dark conductivity of hydrogenated amorphous carbon a-C:H (also referred to as diamondlike carbon films) following irradiation with energetic ion beams [C+ (50 keV), Ar+ (110 keV), and Xe+ (270 keV)] has been reported [44]. This enhancement is only found for fluences above $10^{14}\,\mathrm{ions\,cm}^{-2}$. For doses between 10^{15} and $10^{17}\,\mathrm{cm}^{-2}$, it was found that all the hydrogen is evolved from the a-C:H thin films, resulting in a dramatic increase in the dangling bond density, which provides a conduction channel in the diamondlike carbon films.

TABLE II. Ratio of dark conductivity for a/nc-Si:H films measured at 450 K after (post-) and before (pre-) proton irradiation and the c-Si crystal fraction *Xc* as %, determined by Raman spectroscopy, as a function of proton fluence

	Pad 4		Pad 3		Pad 2		Pad 1	
Proton fluence (cm^{-2})	$\frac{\sigma_{post}}{\sigma_{pre}}$	$X_c(\%)$	$\frac{\sigma_{post}}{\sigma_{pre}}$	$X_c(\%)$	$\frac{\sigma_{post}}{\sigma_{pre}}$	$X_c(\%)$	$\frac{\sigma_{post}}{\sigma_{pre}}$	$X_c(\%)$
10^{15}	27.4	6.7	10.7	2.5	5.7	<1	7.2	<1
2×10^{14}	4.0	6.4	13.3	3.3	4.2	<1	12.8	<1
2×10^{13}	7.9	7.4	4.8	3.9	22.5	<1	4.3	<1

Higher ion doses increase the number and/or size of graphitic microcrystallites eventually leading to transformation of the material to macroscopic graphite, with a significant change in the carbon-bonding sp^2/sp^3 ratio.

The photoconductivity is given by $\sigma_{\rm ph} = G\tau e\mu$, where G is the generation rate due to the incident light intensity and the proportion of light absorbed in the thin film, and τ is the recombination lifetime, which in a-Si:H depends inversely on the dangling-bond density $N_{db}(\tau \sim {N_{db}}^{-1})$ [12,45]. Consequently, an increase in dangling-bond density in the a/nc-Si:H films, similar to what was found for the diamondlike carbon films [44], should be reflected in a significant decrease in the photoconductivity. As shown in Fig. 6(b), while the photoconductivity is reduced for the films exposed to proton fluences of $2 \times 10^{13}\,\mathrm{cm}^{-2}$ and $2 \times 10^{14}\,\mathrm{cm}^{-2}$, pad 4 for the film with an irradiation dose of $10^{15}\,\mathrm{cm}^{-2}$, which exhibited an over an order of magnitude increase in the dark conductivity, has a photoconductivity essentially unchanged from the value found in the preirradiated state. It is unlikely that the enhancement of the conductivity observed here is due to a new conduction channel, such as hopping through a higher density of dangling bonds. It should be noted that, unlike the case of the a-C:H films irradiated with an ion dose $>10^{17}\,\mathrm{cm}^{-2}$, for which a change in bonding structure from sp^3 to sp^2 was found [44], we see no evidence in the Raman spectra for such a transformation in our films.

VI. SUMMARY

We report observations of a permanent enhancement of the dark conductivity of a/nc-Si:H composite thin films when irradiated with 16-MeV protons for fluences $\geqslant 2 \times 10^{13}\,\mathrm{cm}^{-2}$. This improvement in the dark conductivity is not presently understood. There is no clear correlation between the enhanced conductivity and any changes in the activation energy or silicon crystal fraction following irradiation, suggesting that neither an increase in free-carrier concentration nor an increase in charge transport through the nc phase is sufficient to explain our results. Further studies of this phenomenon are underway, in particular testing the possible role of compositional morphology due to the embedded nanocrystals and any changes in long-range electronic disorder with irradiation. Sensitivity of the composite a/nc-Si:H films to irradiation with high-energy electrons and other ions will also be investigated. In addition to elucidating the mechanism responsible for this enhancement, the sensitivity of this effect to various parameters, including the nc diameter, doping level, and chemical composition (such as nc-Ge in a-Si:H or nc-Si in a-Ge:H) will be determined.

ACKNOWLEDGMENTS

This work was supported by NSF Grants No. PHYS-1344251, No. PHY-1712953, and No. DMR1608937, the NINN Characterization Facility, and the University of Minnesota Grant-in-Aid program. Portions of this work were conducted in the Minnesota Nano Center, which is supported by the National Science Foundation through the National Nano Coordinated Infrastructure Network (NNCI) under Award No. ECCS-1542202.

[1] J. Yang, A. Banerjee, and S. Guha, Sol. Energy Mater. Sol. Cells **78**, 597 (2003).
[2] M. Moll *et al.* (The RD50 Collaboration), Nucl. Instrum. Methods Phys. Res. A **546**, 99 (2005).
[3] E. Fretwurst *et al.* (The RD50 Collaboration), Nucl. Instrum. Methods Phys. Res. A **552**, 7 (2005).
[4] D. J. Mazey, R. S. Nelson, and R. S. Barnes, Philos. Mag. **17**, 1145 (1968).
[5] V. N. Bhoraskar, S. D. Dhole, S. Singh, S. M. Jahagirdar, and K. S. Srinivas, Nucl. Instrum. Methods Phys. Res. B **62**, 99 (1991).
[6] M. Alurralde, M. J. L. Tamasi, C. J. Bruno, M. G. Martínez Bogado, J. Plá, J. Fernández Vázquez, J. Durán, J. Schuff, A. A. Burlon, P. Stoliar, and A. J. Kreiner, Sol. Energy Mater. Sol. Cells **82**, 531 (2004).
[7] See, for example, H. Schade, in *Semiconductors and Semimetals Vol. 21: Hydrogenated Amorphous Silicon, Part B, Optical Properties*, edited by J. I. Pankove (Academic Press, New York, 1984).
[8] N. Kishimoto, H. Amekura, K. Kono, and C. G. Lee, J. Nucl. Mater. **258**, 1908 (1998).
[9] M. Kagan, V. Nadorov, S. Guha, J. Yang, and A. Banerjee, *28th IEEE PVSC* (Anchorage, AK, USA, 2000), p. 1261.
[10] N. Wyrsch, C. Miazza, S. Dunand, C. Ballif, A. Shah, M. Despeisse, D. Moraes, F. Powolny, and P. Jarron, J. Non-Cryst. Solids **352**, 1797 (2006).
[11] V. Perez-Mendez, S. N. Kaplan, G. Cho, I. Fujieda, S. Qureshi, W. Ward, and R. A. Street, Nucl. Instrum. Methods Phys. Res. A **273**, 127 (1988).
[12] See, for example, R. A. Street, *Hydrogenated Amorphous Silicon* (Cambridge University Press, Cambridge, 1991).
[13] R. A. Street, J. Zesch, and M. J. Thompson, Appl. Phys. Lett. **43**, 672 (1983).
[14] Y. Adjallah, C. Anderson, U. Kortshagen, and J. Kakalios, J. Appl. Phys. **107**, 043704 (2010).
[15] J. Kuendig, M. Goetz, A. Shah, L. Gerlach, and E. Fernandez, Sol. Energy Mater. Sol. Cells **79**, 425 (2003).
[16] A. Yelon, H. Fritzsche, and H. M. Branz, J. Non-Cryst. Solids **266-269**, 437 (2000).
[17] P. Danesh, B. Pantchev, I Savatinova, E. Liaokapsis, S. Kaschieva, and A. G. Belov, Vacuum **69**, 79 (2003).
[18] Z. Razieli, R. Rusack, and J. Kakalios, *Materials Research Society Symposia Proceedings* (Materials Research Society, Pittsburgh, PA, 2015), Vol. 1770, p. 49.
[19] S-i. Sato, H. Sai, T. Ohshima, M. Imaizumi, K. Shimazaki, and M. Kondo, Nucl. Instrum. Methods Phys. Res. B **286**, 29 (2012).
[20] S-i. Sato, H. Sai, T. Ohshima, M. Imaizumi, and K. Shimazaki, and M. Kondo, J. Non-Cryst. Solids **358**, 2039 (2012).
[21] S-i. Sato, H. Sai, T. Ohshima, M. Imaizumi, K. Shimazaki, and M. Kondo, J. Non-Cryst. Solids **356**, 2114 (2010).

[22] N. Kishimoto, H. Amekura, K. Kono, and C. G. Lee, J. Non-Cryst. Solids **227-230**, 238 (1998).
[23] H. Amekura, N. Kishimoto, K. Kono, and A. Kondo, J. Non-Cryst. Solids **266-269**, 444 (2000).
[24] J. Kakalios and H. Fritzsche, Phys. Rev. Lett. **53**, 1602 (1984).
[25] A. J. Hamed, Phys. Rev. B **44**, 5585 (1991).
[26] H. Mell and W. Beyer, J. Non-Cryst. Solids **59-60**, 405 (1983).
[27] J. K. Nangoi, K. Bodurtha, and J. Kakalios, J. Appl. Phys. **124**, 165102 (2018).
[28] L. Mangolini, E. Thimsen, and U. Kortshagen, Nano Lett. **5**, 655 (2005).
[29] U. Kortshagen, J. Appl. Phys. D **42**, 113001 (2009).
[30] L. Mangolini, J. Vac. Sci. Technol. B **31**, 020801 (2013).
[31] P. Scherrer, Nachr Ges Wiss Göttingen **2**, 96 (1918).
[32] J.M. Essick, Z. Nobel, Y.-M. Li, and M.S. Bennett, Phys. Rev. B **54**, 4885 (1996).
[33] L. R. Wienkes, A. Besaws, C. Anderson, D. Bobela, P. Stradins, U. Kortshagen, and J. Kakalios, *Materials Research Society Symposia Proceedings* (Materials Research Society, Pittsburgh, PA, 2010), Vol. 1245, p. 201.
[34] R. N. Pereira, D. J. Rowe, R. J. Anthony, and U. Kortshagen, Phys. Rev. B **83**, 085449 (2011).
[35] R. N. Pereira, D. J. Rowe, R. J. Anthony, and U. Kortshagen, Phys. Rev. B **86**, 155327 (2012).
[36] M. Tanabashi *et al.* (Particle Data Group), Phys. Rev. D **98**, 030001 (2018).
[37] D. L. Staebler and C. R. Wronski, Appl. Phys. Lett. **31**, 292 (1977).
[38] D. L. Staebler and C. R. Wronski, J. Appl. Phys. **51**, 3262 (1980).
[39] M. Taniellian, Philos. Mag. B **45**, 435 (1982).
[40] E. Flitsiyan, C. Schwartz, L. Chernyak, R. E. Peale, Z. Dashevsky, and W. Vernetson, Radiat. Eff. Def Solids **166**, 104 (2011).
[41] J. Kakalios and R. A. Street, Phys. Rev. B **34**, 6014 (1986).
[42] J. Kakalios, Philos. Mag. Lett. **55**, 129 (1987).
[43] R. Anthony and U. R. Kortshagen, Phys. Rev. B **80**, 115407 (2009).
[44] S. Prawer, R. Kalish, M. Adel, and V. Richter, J. Appl. Phys. **61**, 4492 (1987).
[45] See, for example, A. Rose, *Concepts in Photoconductivity and Allied Problems* (Robert E. Krieger Publishing, Malabar, FL, 1978).